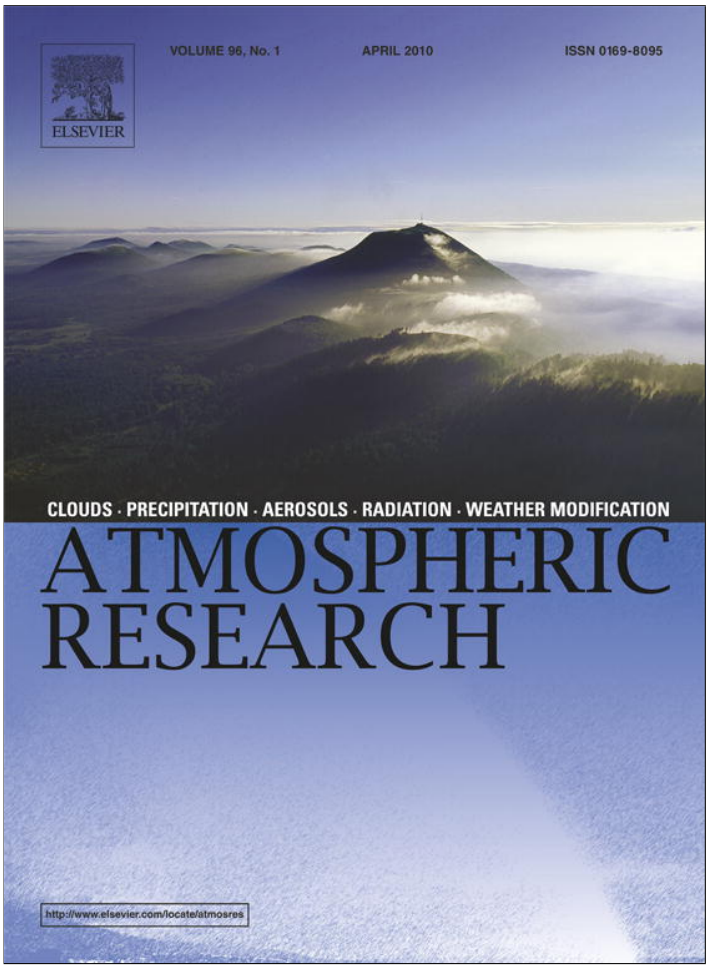

Atmospheric Research 96 (2010) 149–158

Contents lists available at ScienceDirect

Atmospheric Research

journal homepage: www.elsevier.com/locate/atmos

Identifying the scaling properties of rainfall accumulation as measured by a rain gauge network

Michael L. Larsen [a,*], Aaron Clark [b], Matt Noffke [a], Grant Saltzgaber [a], Aaron Steele [c]

[a] Department of Physics and Physical Science, University of Nebraska at Kearney, Kearney, NE 68849, United States
[b] Department of Mathematics and Statistics, University of Nebraska at Kearney, Kearney, NE 68849, United States
[c] Department of Computer Science and Information Sciences, University of Nebraska at Kearney, Kearney, NE 68849, United States

ARTICLE INFO

Article history:
Received 22 May 2009
Received in revised form 9 September 2009
Accepted 17 December 2009

Keywords:
Precipitation
Scaling
Rainfall accumulations
Tipping-bucket

ABSTRACT

Recent studies have revealed that rainfall has non-trivial structure on small (less than 1 km) and short (less than 5 min) spatio-temporal scales. Despite this realization, instruments with substantially poorer resolution are still often used to characterize rainfall accumulations and other rain microphysical parameters such as mean drop diameter, radar reflectivity, and drop size distribution.

There are many recent investigations that have supplied evidence that rainfall may have scale-invariant properties. If this is true, instruments with course resolution should only be trusted to estimate microphysical properties in a spatio-temporal regime where they are able to resolve the scale-invariant nature of the data. Here, we use a small-scale tipping-bucket rain gauge network (an instrument with inherent temporal scale limitations) to identify the minimum and maximum time scales over which a storm's scale-invariant behavior can be resolved. This gives some insight to the minimum time scale of scientific value from this instrument and the technique utilized here can be extended to a variety of other scale-limited raindrop measurement instruments (e.g. Joss-Waldvogel disdrometers, weighing rain gauges, or radar).

1. Introduction and motivation

Rain microphysics has been an active area of research for at least six decades (see, e.g., Marshall and Palmer, 1948). The focus for most of this research has been the measurement and characterization of the rain drop size distribution and its associated moments, as this distribution ultimately can help us understand the dynamics of rain formation and storm evolution (see, e.g., Ulbrich and Atlas, 2002).

The search for the drop size distribution has led to investigations as to how the DSD changes in time and space, which in turn has led to various competing descriptions of the spatio-temporal structure of rainfall. Several papers exist that describe raindrop arrivals as (i) perfectly random in time, characteristic of a Poisson process (e.g. Larsen et al., 2005; Uijlenhoet et al., 2006); (ii) piecewise perfectly random in time, but with a changing mean intensity, characteristic of a so-called inhomogeneous Poisson process (e.g. Jameson, 2007; Uijlenhoet and Sempere-Torres, 2006); (iii) statistically homogeneous or stationary in time, but with non-Poisson statistical structure (e.g. Jameson and Kostinski, 1999; Kostinski et al., 2006); and (iv) scale-invariant and/or with some fractal properties (e.g. Gupta and Waymire, 1990; Ignaccolo et al., 2009; Lovejoy and Mandelbrot, 1985; Peters et al., 2002; Vaneziano et al., 1996; Waymire, 1985; Zawadzki, 1995) including physically motivated scaling theories of rainfall characterization (e.g. Lovejoy et al., 2008; Lovejoy and Schertzer, 2008).

No matter which statistical structure is used to characterize rainfall, there do exist scales beneath which discussion of the DSD becomes nonsensical (see, e.g., Jameson and Kostinski

* Corresponding author.
E-mail address: LarsenML@unk.edu (M.L. Larsen).

0169-8095/$ – see front matter © 2010 Elsevier B.V. All rights reserved.
doi:10.1016/j.atmosres.2009.12.008

2001, 2002b; Kostinski et al., 2006). The argument cuts to the quick of what is meant when referring to a droplet size distribution.

1.1. Notion of scale implicit in drop size distributions

A drop size distribution, in its most current iteration, is understood to be a distribution $p(D)$ (which may be a function of spatial coordinates $\underline{x}$ and time t) and quantifies the relative abundance of raindrops of different diameters D. This is complicated by the fact that every measurement or observation of a DSD occurs over a spatial domain V and a time interval T; all point instantaneous measurements will give either a delta-function like distribution (there is only one drop size at this specific point and at this specific time, namely that of the sole drop in this volume) or — much more commonly — a null result (when the small averaging volume is void of any drops). The introduction of an averaging volume is necessary because the drop size distribution is a concept that only makes sense when describing a space or time interval with at least a certain extent.

Although the abstraction of $p(D)$ defined for every point and time in a field may be of some use when developing our understanding of microphysical processes, ultimately it is an unphysical idealization. The theory is an incomplete description of the reality of the situation since raindrops are finite in number and size, whereas the $p(D)$ formalism is generalized as a field variable that can vary continuously in space and time.

Although the distinction may seem overly formal, it is now clear that we cannot measure $p(D)$ and the associated quantities related to its moments without some temporal and spatial averaging scale becoming relevant. All rain events are fundamentally *finite* both in time and spatial domains and correspond to the arrivals of objects that have physical spatial size and duration. This, too, necessarily invokes some notion of scale into the problem.

Measuring on spatial and time scales that are too small will introduce a "shot-noise" like element into the specification — undersampling will induce neighboring measurements to be different, even if there is no actual difference in the statistical or physical structure of the rain itself. These different measurements may be, in part, due to an actual change in the underlying droplet size distribution. The different adjacent measurements will also be due, in part, to fluctuations about the true measurement caused by inadequate sampling. It has previously been argued (e.g., Larsen et al., 2005) that there is no assumption-free way to determine what fraction of a changing sample-average is due to a change in the actual underlying distribution and what fraction is due to local fluctuations.

To meaningfully talk about DSD change (and changes in associated properties), it would be of use to be able to identify spatial and time scales beyond which we would have some confidence that changes are characterized by physical underlying changes in the distribution. Above it was argued that it is impossible to do this in an assumption-free way, but all hope is not lost if we make some assumptions about the underlying statistical structure of $p(D)$.

1.2. Outline

In an effort to explicitly bring discussion of measurement scales into the discussion of drop microphysics, we present here an analysis of the scaling properties of precipitation accumulation associated with a tipping-bucket rain gauge array. We chose this instrument for study because its spatio-temporal limitations are evident; the time between successive tips of the tipping bucket are obviously longer than the inter-arrival times of drops, the instrument involves some notion of "integration" (no tip occurs unless a certain volume has accumulated), and the spatial extent of the measurement is evident — the surface area of the detector. We also chose this instrument to demonstrate how some scale-invariant properties can still be identified even when using an instrument with scale-based limitations.

In the rest of this paper, we outline the statistical model assumed for drop and tip-arrivals (Section 2 and Appendix A), describe the experimental setup of our study (Section 3), carry out data analysis with our assumed statistical structure (Section 4 and Appendix B), discuss our results (Section 5), and offer suggestions for how this work can be extended and applied to other instruments (Section 6).

2. Assumed statistical structure

Above, we cited several papers that have argued for a statistical description of rainfall that has scale-invariant characteristics. There are a large number of different ways to interpret this statement and we make no claim that the way we interpret this structure here is in any way definitive; rather we offer this statistical description as *a possible* way to characterize the rain statistics.

In particular, here we argue that there is a particular property of the rainfall — as measured — that exhibits a power–law relationship similar to those viewed in fractal system. The validity of this statistical structure can be reasonably questioned; however, if the general statistical structure *does* hold, then we can readily identify some minimum spatio-temporal scales above which we can be confident that the underlying structure of the DSD, or its characteristic moments, is being reliably measured.

The values of the identified minimum scales may depend on the instrument used for the measurements. In this work, we will be utilizing an instrument that has very limited ability to resolve temporal information, thus probably setting limits that are more constrained than would be found with an instrument with finer temporal resolution. However, given the wide availability of tipping-bucket rain gauges, we argue that there is still value in identifying this instrument-dependent lower-bound for the scaling regime. In Appendix A, we do demonstrate that the use of an integrating device like a tipping-bucket rain gauge does reliably maintain some of the scaling properties of the underlying process. That being said, the integrating nature of the tipping-bucket rain gauge does suggest that even though a scaling regime is found, it may or may not be physical in nature.

2.1. Quantities to identify

The purpose of this paper is to try to identify the time scales (based on tipping-bucket accumulations) that can serve as minimum time scales for discussing the DSD of individual storms and how they evolve with the caveat that an assumed scale-invariant statistical structure is appropriate throughout. As tipping-bucket

rain gauges are integrating devices, the time scales are actually upper-bounds on the minimum time scales that can be used. In addition to identifying the time scale corresponding to the beginning of the temporal scaling regime, we also demonstrate that the exponent in the scaling power–law (as measured) seems reasonably insensitive to small spatial offsets for a single storm, but does vary substantially from storm to storm.

2.2. Which variable scales?

Given the proliferation of different statistical models of rainfall, we have chosen a structure that is particularly easy for us to analyze. Following a previous study by Zawadzki (1995) as adapted for cloud particle DSD analysis in Knyazikhin et al. (2005) and Marshak et al. (2005), we will be assuming that:

$$N(\tau) = \alpha\tau^{-D} \tag{1}$$

where $N(\tau)$ is the number of disjoint, successive time intervals of duration τ in the storm containing at least a single tip of a rain gauge. The positive parameters α and D are those of the statistical fit, and τ is a time interval that spans from the smallest time-increment detectable by our recording instrumentation to T, the duration of the storm.

Following the references cited above, it is said that the data has been characterized once α and D have been identified. More important for our goal here is that we specify $\tau_{\min}$ and $\tau_{\max}$, the two temporal scales that identify the minimum and maximum temporal scales (respectively) over which the statistical structure properly describes the data.

The existence of a minimum and maximum time scale over which the scale-invariant properties may occur has been argued for the general case previously (e.g. Kostinski et al., 2006). Given the specific scaling structure proposed here, we can understand the existence of these scales for this application in a more clearly demonstrable way.

Both the existence of $\tau_{\min}$ and $\tau_{\max}$ are inevitable due to the finite nature of the data. Let there be n total tips occurring at times $t_1, t_2, t_3, \ldots t_n$. Further, let the time between tips be measured by $(\Delta t)_i$ where $(\Delta t)_i = t_{(i+1)} - t_i$. By construction, for all $\tau < \min\{(\Delta t)_i\}$, we know that each disjoint interval has no more than 1 tip. Thus, $N(\tau) = n$ for all $\tau < \min\{(\Delta t)_i\}$. Technically, this is a scale-invariant regime with $D = 0$, but this "scale-invariance" is a consequence of only the finite nature of the data and gives us no useful information about the microphysics. Hence, this scale-invariant regime is not the one of interest. Consequently, $\tau_{\min} > \min\{(\Delta t_i)\}$.

Similarly, we can identify a meaningful upper bound for $\tau_{\max}$ as a storm of duration T will inevitably have at least 1 tip in each time interval of duration T, $T/2$, $T/3$, and $T/4$ with $N(T/k) = k$ for $k \lesssim 10$. In this range, we find another "unphysical" scaling regime where $D = 1$. (Both of these non-scaling regimes are discussed in Larsen et al., 2005).

The task at hand, then, is to find a scaling regime outside of these excluded intervals that adequately describe the data in some range of τ. This technique is outlined in Appendix B. An additional complication in this work is that there are actually up to 30 different time series corresponding to 30 different values of $N_k(\tau)$. (See the section below on Experimental setup). Since D, α, $\tau_{\min}$ and $\tau_{\max}$ are intended to describe the rain event as a whole, we used all of the $N_k(\tau)$ to help identify $\tau_{\min}$ and $\tau_{\max}$. The specific algorithm used to select these endpoints is described in detail in Appendix B.

3. Experimental setup

An array of thirty tipping-bucket rain gauges was constructed and arranged in a 5×6 network with grid spacing of 5 ft. These gauges (Spectrum Technologies, Item 3525R) were individually re-calibrated with known volumes of simulated rain to be within a 2% tolerance of real accumulations. Each tip of the gauge — corresponding to 1/100th of an inch of accumulation over an 8 inch diameter circular collecting surface (nominally 8.24 mL of accumulation over the surface) — was recorded using an automated computer acquisition system.

Inside each detector, a 9 V battery and voltage divider were inserted so that a tip, completing a circuit, would supply a known 5 V pulse over a transmission line which could be recorded by our computer fitted with a National Instruments USB-6008 data acquisition board. This gave us exact tipping times (to within 1/40th of a second) for each gauge in the array for each tip.

This acquisition setup was run continually (except for brief periods of instrumental downtime due to extended power outages and when acquisition was turned-off for recalibration) from April through October 2008 on the roof of the Bruner Hall of Science on the University of Nebraska at Kearney campus. Each platform on the grid was independently leveled and checked periodically throughout the summer. There were no obstructions nearby to prevent precipitation accumulation, however the array was near the edge of the roof and, consequently, it is possible some updrafts existed near the edge of the building changing the accumulation on the edge gauges of the array. A picture of the rain gauge array is shown in Fig. 1.

4. Data analysis

A large number of events were recorded. Of these, we selected several for further study when preliminary analysis revealed that there was possible evidence for a "scaling regime" in each of them. Relevant parameters associated with each event are given

Fig. 1. A photograph of part of the rain gauge array used to acquire data in this experiment. Each of the black canisters is calibrated and leveled tipping-bucket rain gauges. Accumulations for each gauge were recorded and analyzed using a customized data-recording system run from a computer in the adjacent penthouse.

in Table 1. Each event lasted at least 2 h (measured from the first to last tip recorded) and corresponded to an accumulation of at least 0.45 in (an average of at least 45 tips per gauge, corresponding to at least modest rainfall rates during the most intense parts of the rain event and enough accumulations to allow for a meaningful analysis of the statistical structure of the time series). A figure demonstrating total accumulations as a function of time for one of the rain events is depicted in Fig. 2.

4.1. Basic statistical properties

In an effort to confirm that our measurements were reasonable, we compared the rainfall accumulations detected by our rain gauge array to the radar estimates from the closest NWS radar (KUEX near Hastings, NE). We asked the personnel at that station to give us the Z–R relationship they used for the storms in question. They supplied the relation $Z = 300R^{1.4}$ for each event we asked about, using Z from a compound scan involving the two lowest elevation angles. After reconstruction for the pixel that the rain gauge network was located in, we compared the observed rain accumulations for each interval to those inferred from the radar (see Fig. 3).

Although the total accumulations between the radar inversion and the rain gauge network often differed by over 30%, we found this to be an acceptable agreement. How can we justify this claim? (1) Z–R inversions are crude; only a single "snapshot"is taken and used to estimate rainfall over an entire pixel (approximately the size of the entire UNK campus) and for the entire scan-time (nominally 4.5 min), substantial variability on time and space scales smaller than this has been demonstrated previously (see, e.g., Jameson and Kostinski, 1999). (2) although the total accumulations do differ, the rain gauge estimates and the radar retrieval do correlate well with each other insofar as both measurements show increased and decreased rainfall intensity at approximately the same times. Finally, (3) we see that most of the difference between the radar inversion and the rain gauge measurements occur in times of heavy accumulation; heavy accumulation is when tipping-bucket rain gauges are known to undercount the most and the Z–R relationship used is most likely to give spurious overestimates (due either to coherent return or a different underlying Z–R relationship) (see, e.g., List, 1988; Jameson and Kostinski, 2002a). Although the undercounting by the rain gauges in heavy rainfall may influence our estimation of the scaling regime, it does not concern us in this study as we are trying to determine the characteristic scale *for the instruments in question*, not necessarily for the physical process directly.

Table 1
Basic summary information for the 5 rain events analyzed here. The Mean accum. is computed by taking the average gauge reading across the network of rain gauges. The duration is computed by calculating the time interval between the first and last recorded tip (even if they are not from the same gauge). $\langle R \rangle$ is the mean rain rate for the event, calculated by taking the mean accumulation divided by the duration and converted to standard units for meteorology. In each of these events, the mean rain rate underestimates the rain rate at the beginning of the event and overestimates the rain rate at the end of the event.

Event	Date (2008)	Mean accum. (in.)	Duration (min)	$\langle R \rangle$ (mm/h)
1	May 27	0.62	171	5.53
2	June 26	0.45	122	5.62
3	July 14	0.68	396	2.62
4	July 16	1.60	235	10.38
5	July 17	1.47	237	9.45

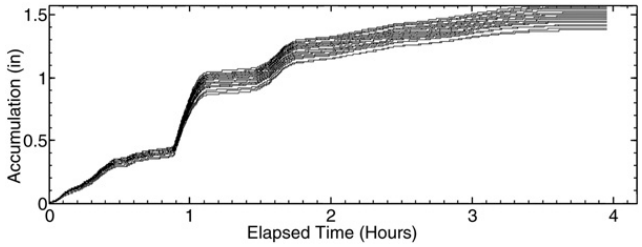

Fig. 2. Total accumulated rainfall as a function of elapsed time for one of the storms investigated in this study. Each line corresponds to the accumulations recorded by an individual rain gauge.

Given the above facts about rain gauge and radar retrieval, we feel confident that our rain gauge network provided a reliable representation (subject to the fundamental limitations of the tipping-bucket rain gauge instrument itself) of the accumulated rainfall for each event.

Qualitative observation of the storms in question does show a clear evolution of the rain event. Most events begin with an intense period of accumulation followed by a transition period and then a period of very mild accumulations. This matches with radar estimates and is a characteristic property of most convective storms in the Great Plains region of the United States. This identifiable progression of storm development does suggest that there may be identifiable DSDs for each part of the storm or even scaling relationships for accumulation that could be identified for each part. However, while the naked eye is seeing a large-scale manifestation of the scale-invariant property, this manuscript is written under the implicit assumption that the time series analysis of the *entire event* is appropriate here.

4.2. Scaling properties — comparison between gauges in a single event

After acquisition, our basic unit for analysis is the individual time series of tip-times for each of the gauges in the array. Often in other work the technique for identifying $\tau_{\min}$ and $\tau_{\max}$ is left unspecified; we describe our technique in detail in Appendix B. The final values of $\tau_{\min}$ and $\tau_{\max}$ found applying this technique

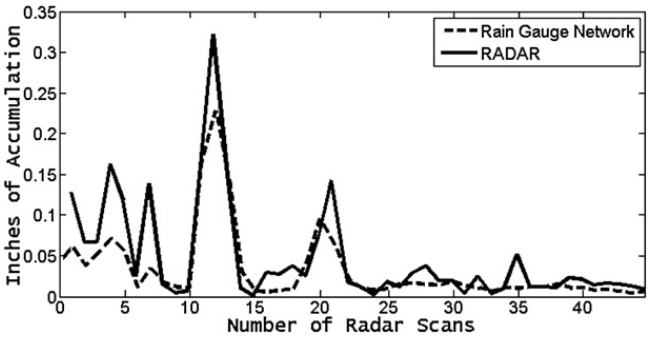

Fig. 3. Comparison between the rain gauge network average accumulations and the KUEX radar inversion of rain accumulations for Event 5. Note the basic agreement in shape, despite the mitigating factors listed in the text. In addition to the disclaimers in the text, it is also worth noting that the rain measured aloft by the radar does not necessarily physically match the rain received on the ground, even if you have an ideal detector (see, e.g., Jameson and Kostinski, 2001). The general agreement shown here is not atypical.

to each of the 5 events chosen for further study are given in Table 2.

Fig. 4 distinctly shows the three ranges evident in each of the N vs. τ curves. For $\tau<\tau_{min}$ (left of the leftmost vertical line), there is almost no slope, suggesting that each tip of the rain gauge occurs in its own disjoint time interval of duration τ. For $\tau>\tau_{max}$ (right of the rightmost vertical line), there is a slope of -1. However, between τ_{min} and τ_{max} there is a regime which sometimes appears linear on a log–log scale with a slope somewhere between 0 and -1. The constant slope of this linear regime suggests a good fit with the statistical model proposed previously.

After identifying τ_{min} and τ_{max} for each event, a least-squares fit on the logarithmically transformed data was used to identify the optimal value of D and α for each gauge. Although α is related to the total accumulation of the event, the variable of most meteorological interest is D. The mean value (averaged over all gauges in the array) and coefficient of variation of D values for each event is also given in Table 2.

Two fits to this linear regime can be identified in Fig. 4. There is a solid line fit based on using the least-squares minimized fit for all of the gauges in the network. The dashed-line fit is optimized only for the gauge in question.

Note both the low coefficient of variation from the mean values of D found for each rain event and the similarity between the solid line fits and the dashed-line fits in Figs. 4 and 5. The closeness of the fits for different rain gauges in the same event is a recurring feature of the data. Fig. 6 shows the different values of D estimated from each gauge in each event.

The above suggests that *the observed values of D and α seem to be characteristic for the accumulation at the entire site and are very similar for closely located rain gauges*. This does not, unfortunately, rule out instrumental effects, since identical instruments were used for all of the measurements. However, it does suggest that *if there is a temporally scale-invariant structure to the rainfall, it is not spatially intermittent on scales smaller than our array*. By this, we mean that the dimension observed seems to be a characteristic of the storm and not of the exact position of measurement. This is promising if we hope to use the scale-invariant parameters to describe the microphysics of a storm or its evolution.

4.3. Scaling properties — comparison between events

If we are to try and use the scale-invariant parameters to describe the microphysics of a storm, it can be argued that we should see some variability in these parameters from storm to storm. Because of this, we set out to measure how much D varies between rain events.

Table 2
Information regarding estimates of D for each of the events. τ_{min} and τ_{max} are the briefest and longest time scales associated with the scale-invariant regimes (as calculated via the methodology described in Appendix B). $\hat{\tau}$ is the mean inter-tip time for the entire event. $\langle D\rangle$ is the estimated value of D for the rain event (averaged among all gauges), and $\sigma(D)/\langle D\rangle$ is the coefficient of variation of the gauge-to-gauge values of D.

Event	τ_{min} (s)	τ_{max} (s)	$\hat{\tau}$ (s)	$\langle D\rangle$	$\sigma(D)/\langle D\rangle$
1	19.8	198.5	165.5	0.558	0.0231
2	49.8	498.8	162.7	0.454	0.0469
3	111.5	1116.5	349.4	0.683	0.0351
4	19.8	198.5	88.1	0.480	0.0231
5	28.0	280.5	96.7	0.465	0.0206

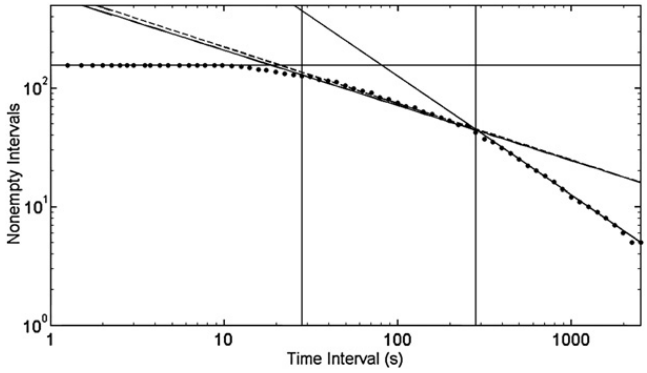

Fig. 4. A plot of $N(\tau)$ vs. τ for Event 5, gauge number 3. The actual data is shown by the circular dots. We see that for $\tau<\tau_{min}$ (approximately 28 s, from Table 2), the data has an essentially horizontal slope. We expect that since few intervals of 28 s or shorter duration can be found with multiple tips. Similarly, for $\tau>\tau_{max}$ (approximately 281 s, from Table 2), the data has a slope very close to -1. We expect this since there are few time intervals of longer than 4 min without at least a single tip. The intermediate regime shows some evidence for scale-invariant behavior. Two fits are shown on this figure. The solid line fit in the intermediate time range corresponds to the average fit for all gauges for this rain event. The dotted-line fit (very close to the solid line fit) is customized for this particular gauge, given the two endpoints that were established by carrying out the minimization schema suggested in Appendix B.

Following the procedure outlined in the previous section and Appendix B, we analyzed the rain accumulations for every operating gauge in each of the 5 events presented in Table 1. For each event, we identified τ_{min}, τ_{max}, $\overline{D}$, and examined the spread from gauge to gauge about $\overline{D}$,. Our results are summarized in Table 2.

Fig. 6 displays the results from each of the gauges from each of the 5 rain events. We notice that, as asserted in the previous section, each rain event has a compact spread about the average value of D reported; each gauge in each event is a reasonably good estimator of D for the process. Perhaps more importantly, however, we note that there are sometimes substantial differences in D from one event to the next. This suggests that knowledge of D (perhaps along with τ_{min} and

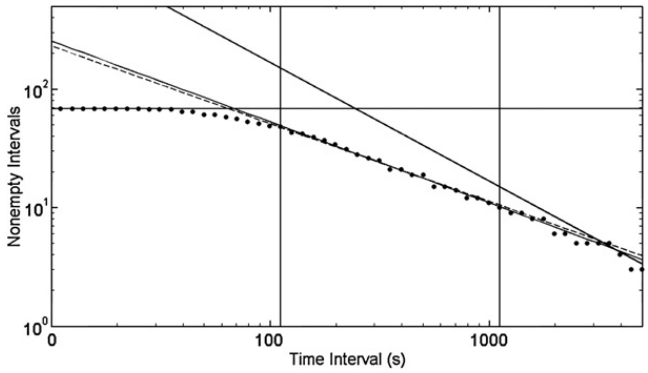

Fig. 5. Similar to Fig. 4, except for Event 3, gauge number 18. Note here that the transition times τ_{min} and τ_{max} are substantially longer in duration. This data-event is a bit more patchy on long time scales, thus we do not see the convergence to the -1 slope until the very end of the division of data shown (nominally 1 h). Note, however, the consistent excellent agreement between the optimized fit for all gauges and the fit customized for this particular gauge.

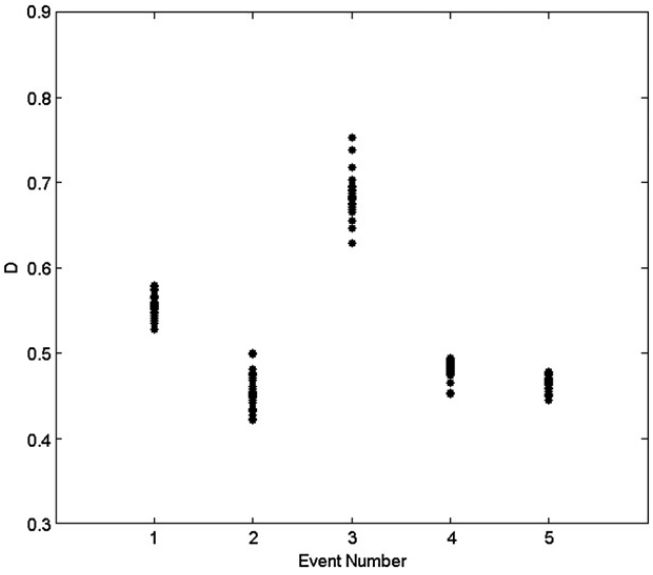

Fig. 6. The individual values of D estimated for each of the gauges for the individual events. We see reasonably tight bunching around the mean value of D for each event (supported by the calculation of $\sigma(D)$ in Table 2). There are, however, substantially different values of D found for the different rain events, suggesting perhaps different fundamental structures to the rainstorm structure and/or microphysics.

τ_{max}) may be able to tell us something about the underlying structure or microphysics of the rain event.

Generally, we expect dimensions that are closer to unity to exhibit fewer clustering characteristics — more uniform rain (see, e.g., Marshak et al., 2005). The uniformity (or lack thereof) of rainfall can be meteorologically relevant for estimating the DSD, retrieving rain rates from radar, and determining spatial variability (Kostinski et al., 2006). However, merely examining the time series of these individual events (no matter what averaging time scale is used) reveals what seems to be a highly intermittent behavior for all the events. Without a scale-invariant analysis like that supplied here, it would be hard to definitively argue that Event 3 shows the most statistical similarity to a perfectly steady rainfall.

5. Discussion

The data presented here, though limited both in quantity and by our adherence to a parametrically simplistic model, is highly suggestive. Given that there is no consensus in the community regarding even the statistical nature of rain, our goal here is not to advocate for a particular model but rather to consider the impact on a model's parameters due to the measurement process.

As is shown in Appendix A, there are certain properties of the actual physical process that still are retained when subject to measurement by our instrumentation. Although there is currently no definitive way to ascertain which properties are retained, examination of the data at hand reveals some noteworthy possibilities meriting further study.

5.1. Spatial variability

The agreement of all the fitting parameters between gauges in the same storm suggests that there is some degree of spatial uniformity regarding the statistical structure of the accumulations on the dimensions associated with the spatial scale of the array. There have been many previous studies (e.g., Jameson and Kostinski, 1999; Lavergnat and Gole, 1998) that have argued that there exists non-negligible spatial clustering on these scales, yet we do not see a great deal of variability in the model fit parameters. This suggests either that (i) this model is not robust enough to capture the variability on these scales (possible, given that the fits occur in log-space and may miss structure on some particular scales), or (ii) the statistical structure is such that though some aspects of the rain do vary on these scales, the accumulation statistics for a typical storm — when measured through an integrating device — do not resolve them. Depending on the meteorological variable of interest, this may or may not be a weakness of the instrument.

5.2. Interstorm variability

The variability in the fitting parameters α and D from storm to storm suggests that perhaps this model, despite being reasonably simple, may be capturing meteorologically meaningful information that is not easily identified via other techniques. The authors attempted to try and categorize the different α and D values based on total accumulations, variances between total gauge accumulations, and variance/mean ratios for total gauge accumulations with no success. Typically, fractal investigations argue that values of D near zero correspond to more of a clustered data-set (see, e.g., Knyazikhin et al., 2005; Marshak et al., 2005), yet an examination of the time series (binned at several different time scales) do not clearly reveal this structure to the naked eye. Perhaps, by using D and α, storm age or structure can be identified. More data, however, would be required to do this in a meaningful way.

5.3. Relationship between τ_{min}, τ_{max} and other parameters

A quick glance at Table 2 reveals a very suggestive trend: we find that $\tau_{\min}<\hat{\tau}<\tau_{\max}$ where $\hat{\tau}=\langle\{(\Delta t)_i\}\rangle$, the mean inter-tip time. Given the data-set at hand, there are only three true time scale parameters that naturally arise from the instrumentation — δt (the time resolution of tip-times, here 0.025 s), $\hat{\tau}$, and T (the duration of the event). Both δt and T are, for both physical and data-analysis reasons, well divorced from both $\tau_{\min}$ and $\tau_{\max}$. However, the existence of $\hat{\tau}$ within the scaling regime is extremely suggestive.

On one hand, it has previously been pointed out (in a slightly different context in Larsen et al., 2005) that the transition from the artificial $D=0$ scaling and the equally artificial $D=1$ scaling must occur in the time range approximately around $\hat{\tau}$, with the reasoning based on the rapid change in the void probability distribution function around $\hat{\tau}$ for all but the most pathological waiting time distribution functions. On the other hand, the fact that we see a well-fit portion of the $N(\tau)$ spectrum near $\hat{\tau}$ for different values of $\hat{\tau}$ in different events suggest that perhaps the scaling behavior exists for a wide range of times that the instruments being used here are not able to resolve due to the poor temporal resolution, the integrating nature of the instrument, and the finite nature of the data.

Future work with other instruments not subject to quite as poor resolution and not of an averaging-type may be able to better determine whether or not the scaling occurring over an order of magnitude always including $\hat{\tau}$ as seen here is a spurious result based on analysis or some real scaling phenomena.

6. Directions for future work

The rain gauge network developed for this study, though with its limitations, has substantial promise in investigating the properties of DSD evolution and storm development.

Pending additional funding, we hope to set up other rain gauge arrays similar to the one described here, to better characterize whether the observed values of D vary from array to array in networks that are 100 m, 1 km, and 10 km apart. This will help identify whether or not D (as measured by rain gauges) is an evolutionary parameter within a storm or characteristic of a storm from origin to dissipation.

Other instruments under development and commercially available (including, in particular, various drop disdrometers) with different limitations should be exposed to the same technique outlined here to determine how $\tau_{\min}$, $\tau_{\max}$, α, and D vary as detected by those instruments. This will help both bound the instrumental influence on estimating D and determine the full scaling regime.

To adapt this approach to another instrument, one needs to adopt the following general strategy. (1) Identify some variable which is naturally counted discretely with good temporal precision (here these are tips of the tipping-bucket; in disdrometers it could be the arrival of individual drops and with radar returns it could be scan-times where returns exceed a threshold). (2) Plot the appropriate variable's non-empty time-interval number on a log scale as a function of time (similar to Figs. 4 and 5) and proceed with the fitting algorithm as described in Appendix B. (3) Develop a heuristic to determine which range of D may be acceptable without inadvertently including the discrete limits near $\tau_{\min}$ and $\tau_{\max}$. (4) Verify that $\tau_{\min}$ is separated from $\tau_{\max}$ by at least an order of magnitude. (5) When possible, try to determine any influences the measuring technique may have on the reported values of D and α.

Finally, it would be useful to link D to other meteorologically relevant information like storm type, age, and structure similar to the work previously done with other variables by Ulbrich and Atlas (2002).

Acknowledgements

The authors would like to thank Robert Price, Steve Eddy, and Rick Ewald for helpful discussions and experimental support. Support for this work was supplied by the Research Services Council at the University of Nebraska at Kearney in the forms of a mini grant (MLL) and a University Research and Creative Activity award (AC and MLL). Additional support for this work was supplied by a NASA Nebraska Space Grant mini grant (MLL) and UNK undergraduate research fellowships (MN, GS, AS).

Appendix A. Justification of scaling behavior

The goal of this Appendix is to demonstrate that integrating devices like the tipping-bucket rain gauge do reflect scaling behavior of underlying processes divorced from direct physical interpretation in terms of our instrumentation.

To this end, we consider two abstract time series $\mathcal{D}=\{d_1, d_2, ..., d_r\}$ and $\mathcal{T}=\{t_1, t_2, ..., t_s\}$ (corresponding to drop and tip occurrence times) which are related by accumulation. That is, there exists a fixed critical quantity $V_c>0$ and, for each $d_i \in D$, an associated positive quantity $V(d_i)$, such that

$$t_i = min\{d_j | \sum_{k=1}^{j} V(d_k) \geq i \cdot V_c\}.$$

Let $\mathcal{A}=\{a_1, a_2, ..., a_p\}$ be an arbitrary time series. For ease of reference, let p denote the number of elements in $\mathcal{A}$ and $T=a_p-a_1$ the duration. Given a time interval $[u, v)$, let

$$\mathcal{I}(\mathcal{A}, [u, v)) = \begin{cases} 1 & \text{if } \{k | u \leq a_k < v\} \neq \varnothing \\ 0 & \text{otherwise} \end{cases}$$

Using this notation, define the *box-counting number at scale* τ as

$$N(\mathcal{A}, \tau) = \sum_{k=1}^{\lfloor \frac{T}{\tau} \rfloor} \mathcal{I}(\mathcal{A}, [(k-1)\tau, k\tau)).$$

We can now rephrase our purpose here with some precision: if we know something about the scaling properties of $N(\mathcal{D}, \tau)$ for $\tau \in [\tau_{\min}, \tau_{\max}]$, what can we say about the scaling properties of $N(\mathcal{T}, \tau)$? We are particularly interested in the answer to this question when, for positive parameters α and D,

$$N(D, \tau) = \alpha \cdot \tau^{-D} \tag{A1}$$

for $\tau \in [\tau_{\min}, \tau_{\max}]$. As a step towards the resolution of this question, we consider three different examples for D where a scaling regime $[\tau_{\min}, \tau_{\max}]$ exists such that Eq. (A1) holds. In

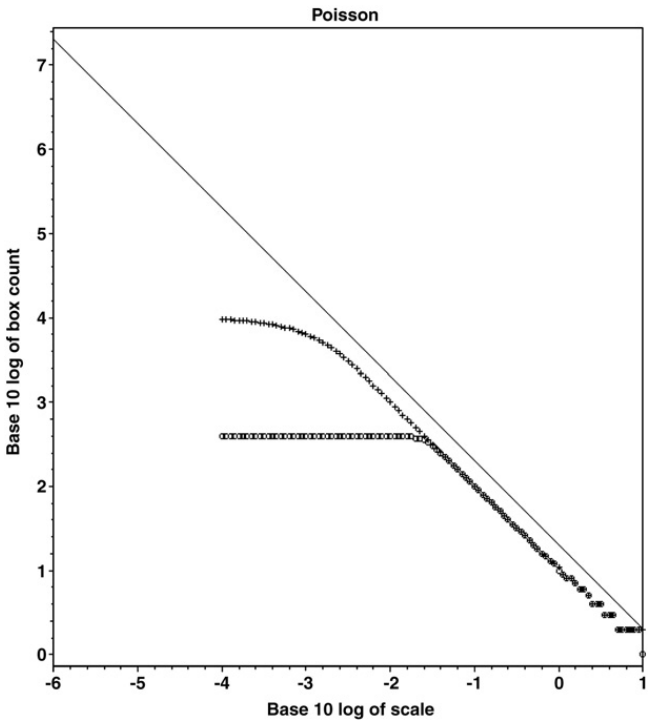

Fig. 7. Simulation of D and $\mathcal{T}$ using a Poisson process. A total of 10,000 d_i are uniformly randomly placed in the interval [0, 1] and assigned positive quantities $V(d_i) = \frac{4}{3}\pi r_i^3$ where r_i is the i-th observation of a uniform random variable on (0, 1). (This assignment of r_i is not meant to be representative of real rain, but has been chosen for its easy implementation and to avoid unnecessary complication).

these examples, the elements of D are derived from a Poisson process, a Matérn cluster process, and a 1-dimensional Lévy flight, and an element of T is found when the accumulated volume V_c exceeds 25 (arbitrary units).

Each example features a duration of 1 time unit. Figs. 7, 8, and 9 depict the box-counting numbers for D (crosses) and T (circles) for scale values ranging from 1 down to 10^{-5} by $10^{-i/20}$, $0 \le i \le 100$ (yielding 20 sample points/decade on the log–log graphs). A reference line of slope -1 is also shown in this group of figures, drawn through the data point $(\log_{10}(d_1), \log_{10}(N(\mathcal{D},1)) = (\log_{10}(d_1), 0)$.

In each example, we observe the expected agreement between $N(\mathcal{D},\tau)$ and $N(\mathcal{T},\tau)$ over scale ranges $\tau < \tau_{\min}$ (where both counts become constant with respect to scale), and $\tau > \tau_{\max}$. In the Poisson example, the counts strictly agree until $\log_{10}(\tau) \approx -1.6$, at which point $N(\mathcal{D},\tau)$ becomes constant. In the Matérn and Lévy examples, we observe that the scaling of $N(\mathcal{T},\tau)$ closely follows that of $N(\mathcal{D},\tau)$ over non-trivial ranges of $\log_{10}(\tau)$: $-2.2 < \log_{10}(\tau) < -.6$ for the Matérn series, and $-2.2 < \log_{10}(\tau) < -.6$ for the Lévy series.

These observations are suggestive of the following: if $N(\mathcal{D},\tau)$ scales as in Eq. (A1) for $\tau \in [\tau_{\min}, \tau_{\max}]$, then there exist positive parameters α' and D' and scales $\tau'_{\min}$ and $\tau'_{\max}$ such that $N(\mathcal{T},\tau) = \alpha' \cdot \tau^{-D'}$ for τ $[\tau'_{\min}, \tau'_{\max}]$.

Given that $N(D,\tau)$ is an abstraction of a theoretical scaling regime for the arrival of individual drops and $N(\mathcal{T},\tau) = \alpha' \cdot \tau^{-D'}$ can be interpreted as the scaling regime associated with tip-times, the results of this Appendix suggest that one would expect a scaling regime for the tipping-bucket data if it inherently exists in the raw data.

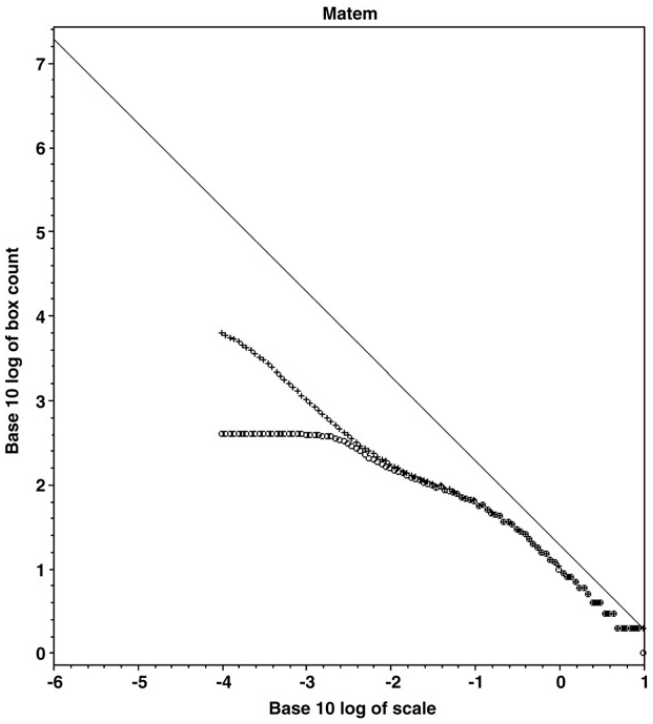

Fig. 8. Simulation of $\mathcal{D}$ and $\mathcal{T}$ using a 1 dimensional Matérn process. A total of 100 parent locations are uniformly randomly selected in the interval [0, 1]. The i-th parent location produces c_i offspring, where c_i is the i-th observation of a Poisson random variable with mean 100. Each of the c_i children are uniformly randomly placed within .005 units of the parent location. The collection of the children becomes the series $\mathcal{D}$ (the parents themselves are not included). As with the Poisson simulation, each d_i is assigned positive quantities $V(d_i) = \frac{4}{3}\pi r_i^3$ where r_i is the i-th observation of a uniform random variable on (0,1).

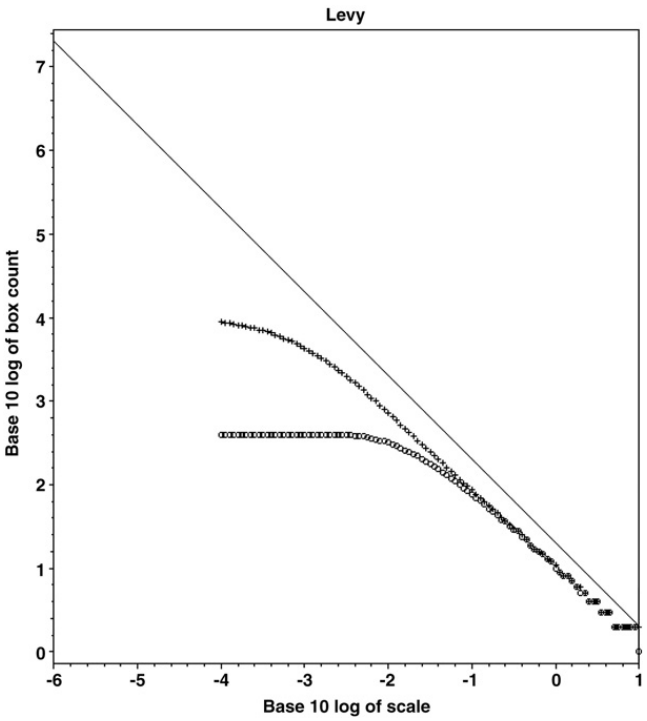

Fig. 9. Simulation of $\mathcal{D}$ and $\mathcal{T}$ using 10,000 steps of a 1-dimensional Lévy flight. Step size follows a power–law distribution αr^k with $k = 1.35$ and $\alpha \approx .00082$, and $.005 < r < .05$. As above, each d_i receives an assigned positive quantity $V(d_i) = \frac{4}{3}\pi r_i^3$ where r_i is the i-th observation of a uniform random variable on (0, 1).

Appendix B. Outline of fitting algorithm

The fitting procedure used in this paper is similar to that found in other investigations in both cloud physics (e.g., see Knyazikhin et al., 2005; Marshak et al., 2005) and precipitation (see, e.g., Larsen et al., 2005; Zawadzki, 1995). In using a box-counting technique to estimate the scaling parameter D, however, care must be taken to only include the observations that are not "tainted" by the finite nature of all measured data. In the plots of non-empty intervals $N(\tau)$ vs. time interval τ, we necessarily see at least three different regimes.

For small τ, we find $N(\tau) = N_0$, the total number of rain gauge tips. The slope of the graph in this regime is, by necessity, 0. No matter how short the temporal division, no more non-empty intervals will be revealed beneath a certain value of τ.

Similarly, for large τ we find that $N(\tau) = \mathcal{T}/\tau$ where T is the total duration of the observation. Simply stated, if one observes a 3 h rain event and examines disjoint sub-intervals of 1 h duration, either 3 intervals with a tip are found or the rain event was not properly characterized as 3 h long. (In the event of fewer than 3 non-empty intervals, one has either 2 rain events of at most 1 h duration with an hour between them or a rain event that really was at most 2 h in total duration).

Finally, between these regimes where the slope is 0 (short τ) and -1 (long τ) there is another, transitional regime. It is in this regime only where there might be some evidence for statistical scale-invariance. Unfortunately, even if the scaling regime formally does physically exist, there will be some range of temporal scales where the finite effects outlined above continue

to have some influence on the N vs. τ curve. As has been noted elsewhere (Larsen et al., 2005), there is no definitive technique to identify when one is at a temporal scale well-represented by the scale-invariant formalism. The technique outlined here is not perfect, but it is important to explicitly identify the method used to specify the minimum and maximum scales where the scale-invariant regime can be identified.

We undertake this task by applying an iterative technique: first, we find the optimal fit suitable for each gauge subject to each possible endpoint pair. Then, we average the different fits for each endpoint pair across all gauges. For each selected endpoint pair, we then use this average fit and minimize the average least-squares deviation per data point over all gauges to find the optimal endpoint pair combination.

To this algorithm, it was necessary to add in the constraints that the measured values of D cannot be outside of the range $0.2<D<0.8$ (to prevent the algorithm from finding the better fit (but unphysical) regions of scale-invariance due to finite data effects). It was also required that the scale-invariant region exist at least over a full order of magnitude (i.e., 20 different values of τ for our data processing technique).

The scale-invariant assumption requires that $N(\tau)$ and τ are related via

$$N(\tau) = \alpha\tau^{-D} \tag{B1}$$

with D taking on some value between 0 and 1. (Values closer to 1 indicate more uniform accumulations in time and values closer to 0 suggest more "clumpy" or "patchy" accumulations).

First, we take the logarithm of the above relationship to obtain:

$$log(N(\tau)) = -Dlog\tau + log\alpha. \tag{B2}$$

Let $0<\tau_1<\tau_2<\ldots<\tau_\mu=T$ be an arbitrary partition of the duration T of an event into time scales. Here we assume $\mu\sim100$ and that between t_i and t_{i+20} there is an order of magnitude difference in scale, as in our data processing technique outlined previously. Note that, for each value of τ, there are actually up to 30 different possible values for $N(\tau)$ (a different value of $N(\tau)$ for each gauge); we will specify these by $N_k(\tau)$. Finally, let I and J be scale indices satisfying $21\le I+20<J\le\mu$.

For each of the k gauges and for each pair of indices I and J satisfying the previous inequality, let $D_k(I,J)$ and $\alpha_k(I,J)$ denote the quantities which realize

$$\min_{D,\alpha}\left\{\sum_{i=I}^{J}\left(log(N(\tau_i))-(-Dlog\tau_i + log\alpha)\right)^2\right\} \tag{B3}$$

for a given pair I, J and gauge k. We record $D_k(I,J)$ and $\alpha_k(I,J)$ as entries in $m\times n\times k$ arrays where m is the number of possible values for I, n is the number of possible values for J, and k is the number of gauges used for the analysis. We then construct the $m\times n$ arrays $\overline{D}$ and $\overline{\alpha}$ via

$$\overline{D}(I,J) = \frac{1}{k}\sum_{\ell=1}^{k} D_\ell(I,J), \tag{B4}$$

and

$$\overline{\alpha}(I,J) = \frac{1}{k}\sum_{\ell=1}^{k} \alpha_\ell(I,J). \tag{B5}$$

After going through this process to find a reasonable fit across all gauges for D and α, we then find the best combination of endpoints to minimize the least squared deviation from the fit. We do this by finding

$$\min_{I,J}\left\{\frac{1}{(J-I+1)}\sum_{i=I}^{J}\sum_{\ell=1}^{k}\left[log(N_\ell(\tau_i))-\left(-D(I,J)log\tau_i + log\ \alpha(I,J)\right)\right]^2\right\}, \tag{B6}$$

and assigning to I_g and J_g the values which minimize this expression. Note that, in finding these minimums, we are considering only pairs I and J for which the corresponding $\overline{D}(I,J)\in(.2,.8)$. $N_k(\tau_i)$ is the observed number of non-empty intervals from gauge k at time interval length τ_i. I_g and J_g indicate the minimized global values for the endpoints of the fit. Our ultimate goal of finding $\tau_{\min}$ and $\tau_{\max}$ has been satisfied — they are τ_{I_g} and τ_{J_g} respectively. After using this minimization to choose a global I and J to be used for *all* gauges, we then record and analyze the statistics relevant to the selection of each gauge:

$$D_k(I_g,J_g) = D_k, \tag{B7}$$

and

$$\alpha_k(I_g,J_g) = \alpha_k, \tag{B8}$$

at which point we will investigate the spread and structure of D_k and α_k for various values of k within a storm and between storms.

References

Gupta, V.K., Waymire, E., 1990. Multiscaling properties of spatial rainfall and river flow distributions. Journal of Geophysical Research 98, 1999–2009.

Ignaccolo, M., DeMichele, C., Bianco, S., 2009. The droplike nature of rain and its invariant statistical properties. Journal of Hydrometeorology 10, 79–95.

Jameson, A.R., 2007. A new characterization of rain and clouds: results from a statistical inversion of count data. Journal of Atmospheric Sciences 64, 2012–2028.

Jameson, A.R., Kostinski, A.B., 1999. Fluctuation properties of precipitation. Part IV: Fine scale clustering of drops in variable rain. Journal of Atmospheric Sciences 56, 82–91.

Jameson, A.R., Kostinski, A.B., 2001. What is a raindrop size distribution? Bulletin of the American Meteorological Society 82, 1169–1177.

Jameson, A.R., Kostinski, A.B., 2002a. Spurious power–law relations among rainfall and radar parameters. Quarterly Journal Royal Meteorological Society 128, 2045–2058.

Jameson, A.R., Kostinski, A.B., 2002b. When is rain steady? Journal of Applied Meteorology 41, 83–90.

Knyazikhin, Y., Marshak, A., Larsen, M.L., Wiscombe, W.J., Martonchik, J.V., Myneni, R.B., 2005. Small-scale drop size variability: impact on estimation of cloud optical properties. Journal of Atmospheric Sciences 62, 2555–2567.

Kostinski, A.B., Larsen, M.L., Jameson, A.R., 2006. The texture of rain: exploring stochastic micro-structure at small scales. Journal of Hydrology 328, 38–45.

Larsen, M.L., Kostinski, A.B., Tokay, A., 2005. Observation and analysis of steady rain. Journal of Atmospheric Sciences 62, 4071–4083.

Lavergnat, J., Gole, P., 1998. A stochastic raindrop time distribution model. Journal of Applied Meteorology 37, 805–818.

List, R., 1988. A linear radar reflectivity–rainrate relationship for steady tropical rain. Journal of Atmospheric Sciences 45, 3564–3572.

Lovejoy, S., Mandelbrot, B.B., 1985. Fractal properties of rain and a fractal model. Tellus 37A, 209–232.

Lovejoy, S., Schertzer, D., 2008. Turbulence, rain drops, and the l**1/2 number density law. New Journal of Physics 10, 075017 doi:075010.071088/071367-072630/075010/075017/075017, 075032pp.
Lovejoy, S., Schertzer, D., Allaire, V., 2008. The remarkable wide range spatial scaling of TRMM precipitation. Atmospheric Research 90, 10–32.
Marshak, A., Knyazikhin, Y., Larsen, M.L., Wiscombe, W.J., 2005. Small-scale drop size variability: empirical models for drop size-dependent clustering in clouds. Journal of Atmospheric Sciences 62, 551–558.
Marshall, J.S., Palmer, W.M., 1948. The distribution of raindrops with size. Journal of Meteorology 5, 165–166.
Peters, O., Hertlein, C., Christensen, K., 2002. A complexity view of rainfall. Physical Review Letters 88, 018701.
Uijlenhoet, R., Sempere-Torres, D., 2006. Measurement and parameterization of rainfall microstructure. Journal of Hydrology 328, 1–7.
Uijlenhoet, R., Porra, J.M., Sempere-Torres, D., Credutin, J.D., 2006. Analytical solutions to sampling effects in drop size distribution measurements during stationary rainfall: estimation of bulk rainfall variables. Journal of Hydrology 328, 65–82.
Ulbrich, C., Atlas, D., 2002. On the separation of tropical convective and stratiform rains. Journal of Applied Meteorology 41, 188–195.
Vaneziano, D., Bras, R.L., Niemann, J.D., 1996. Nonlinearity and self-similarity of rainfall in time and a stochastic model. Journal of Geophysical Research 101, 26371–26392.
Waymire, E., 1985. Scaling limits and self-similarity in precipitation fields. Water Resources Research 21, 1271–1281.
Zawadzki, I., 1995. Is rain fractal? In: Kundzewicz, Z.W. (Ed.), New Uncertainty Concepts in Hydrology and Water Resources. Cambridge University Press, New York.